

# Validation of a track repeating algorithm for intensity modulated Carbon therapy with GEANT4

Qianxia Wang<sup>1,2,\*</sup>, Antony Adair<sup>1,2</sup>, Yu Deng<sup>3</sup>, Hongliang Chen<sup>3</sup>, Michael Moyers<sup>3</sup>, James Lin<sup>3</sup>, and Pablo Yepes<sup>1,2†</sup>

<sup>1</sup>*Department of Physics and Astronomy, MS 315,*

*Rice University, 6100 Main Street, Houston, TX 77005, USA and*

<sup>2</sup>*Department of Radiation Physics, Unit 1420, The University of Texas MD Anderson Cancer,*  
*1515 Holcombe Blvd., Houston, TX 77030, USA*

(Dated: November 9, 2021)

The Fast Dose Calculator (FDC), a track repeating algorithm Monte Carlo method was initially developed for proton therapy. The validation for proton therapy has been demonstrated in a previous work. This method can be expanded to ion applications. Our purpose of this paper is to validate the FDC for carbon therapy. We compare the 3D dose distributions and dose-volume-histograms (DVH) for carbon calculated by FDC with a full Monte Carlo method, GEANT 4. 19 patients in total will be discussed, including 3 patients of prostate, 5 of brain, 3 of head and neck, 4 of lung and 4 of spine. We use gamma-index technique to analyse dose distributions and we do dosimetric analysis for DVH, a more direct and informative quantity for planning system assessment. The FDC calculations of both quantities agree with GEANT4. The gamma-index passing rates of all patients discussed in this paper are above 90% with the criterion 1%/1 mm, above 98% with the criterion 2%/2 mm and over 99.9% with the criterion 3%/3 mm. The Root Mean Square (RMS) of percent difference of dosimetric indices  $D_{02}$ ,  $D_{05}$ ,  $D_{50}$ ,  $D_{95}$  and  $D_{98}$  are 0.75%, 0.70%, 0.79%, 0.83% and 0.76%. And all the difference are allowed for clinical use.

PACS numbers: 34.80.Lx, 52.20.Fs

## I. INTRODUCTION

Particle therapy (Wilson 1946, Amaldi 2005) is considered to have a greater potential to spare healthy tissue than traditional photon-therapy. It can deliver dose to deep-seated or radioresistant tumors and cause less toxicity to the healthy tissue around the tumor (Castro *et al* 2004, Schulz-Ertner *et al* 2007, Ohno 2013, Poludniowski *et al* 2015). Thus in the last few years the number of particle therapy facilities has significantly increased (PTCOG website), in spite of their cost and technological challenges (Newhauser *et al* 2015). Compared with proton therapy, carbon therapy produces narrower lateral penumbra, which allows to minimize damage healthy tissue in the proximity the tumor. Moreover, carbon ions have higher relative biological effectiveness (RBE) than protons (Kraft 2000). This feature causes more DNA double strand breaks and lead to more non-repairable damage to tumor cells. Even though the cost of carbon therapy is 2-3 times more than proton therapy, these advantages has boosted its clinical use. Moreover, good clinical results with carbon therapy have been reported (Schulz-Ertner *et al* 2004, Tsujii *et al* 2004).

An essential component of any particle therapy treatment planning system is the dose calculation engine. Traditionally dose calculations was carried out with Pencil Beam Algorithms (PBS) (Petti 1992, Russell *et al* 1995, Hong *et al* 1996, Deasy 1998, Schneider *et al* 1998, Schaffner *et al* 1999, Szymanowski and Oelfke 2002, Taylor *et al* 2017), due to their calculation speed. However, it has been shown that Monte Carlo algorithms provide higher accuracy, especially in areas with large homogeneities (Taylor *et al* 2017). Traditional Monte Carlo code require calculations times orders of magnitude larger than PBS algorithms. However, in the last few years a variety of faster Monte Carlos have been developed (Yepes *et al* 2009a, b, Dallas MC, Mayo MC, whatever else we can found). Among them, the only fast Monte Carlo for ion therapy is (Mayo).

Among the fast Monte Carlos, the Fast Dose Calculator (FDC), a track-repeating Monte Carlo algorithm for protons was developed by Yepes *et al.* (Yepes *et al* 2009a, b), which can increase the calculation speed with respect to traditional MC by few orders of magnitude. FDC was validated versus full Monte Carlo, GEANT4, for proton therapy in (Yepes *et al* 2016) In this work, we report in the extension of FDC to ion therapy and its validation.

---

\*Electronic address: qwl14@rice.edu

†Electronic address: yepes@rice.edu

## II. METHODS

### III. FDC EXTENSION TO IONS

A stand-alone code, referred to as GEANT4, based on GEANT4 version 10.1.0 (Agostinelli *et al* 2003, Allison *et al* 2006), with the physics list FTF\_BERT was used for two purposes. Firstly it was utilized to generate the database of trajectories of carbon ions,  $C^{12}$ , in water that was used as an input for FDC. Secondly it was employed to generate the reference dose distributions for treatment plans for validation.

The database of  $C^{12}$  trajectories in water was generated by simulating 10K carbon ions with an energy of 5200 MeV impinging on a water phantom with the dimension of  $510 \times 510 \times 2500$  mm<sup>3</sup>. For each impinging carbon, all the particles (ions, protons, neutrons, electrons, and gammas) produced from it were stored. In addition, all the steps of the original particle and of all its daughters were recorded in the database, along with the energy loss, the length, and direction for each step.

In addition to the trajectory database, parameters to scale the step length for different particles and materials were calculated and stored in a parameter repository. Similarly to the proton case, we considered a list of 49 biological and other materials commonly encountered in radiation therapy (lucite, brass, etc). For each material and a charged particle (ions, protons, and electrons), a table of the Relative Stopping Power (RSP) was stored as a function of particle kinetic energy in 1 MeV steps. RSP is defined as the stopping power of the material relative to water. The stopping power was obtained from the method ComputerTotalDEDX from G4EmCalculator for each particle, material and particle energy.

As for protons (Yepes *et al* 2016), the particle scaling parameters for scattering angles were obtained by taking the ratio of the scattering angle in the material relative to water. However, this was implemented as function of particle energy in 1 MeV steps, while in previous versions of the algorithm ratios were averaged over particle energies. Scattering angles of particles through a uniform slab of materials of thickness  $0.02$  g/cm<sup>2</sup> were calculated with the Moliere approximation, as implemented by Lynch and Dahl (1991).

The basic track-repeating principle in FDC remains as in the proton case (Yepes 2009 a, 2009 b). However, the algorithm was updated to handle ions by utilizing the extended parameter repository with the length and angle scaling parameters for ions produced in carbon collisions, as explained in the previous section.

### IV. PATIENT COHORT

We selected 19 patients from different clinical sites treated at the University of Texas MD Anderson Cancer Center (MDACC) with Intensity Modulated Proton Therapy (IMPT). The five clinical sites include prostate, brain, head & neck, lung and spine. For each type, 2 to 5 patients were selected for the study in this paper. The retrospective planning or dose calculations studies are conducted within purview of a generic protocol approved by an MD Anderson Internal Review Board.

Since we did not have clinical ion plans available to us, we started with clinically used proton plans, and converted them into carbon treatment plans. Such conversion was achieved by replacing for each energy layer the proton phase-space files describing the proton beam with carbon phase-space files, where protons of a given range were replaced with carbons ions with the same range. Obviously, the dose distributions for the proton and carbon plans are not exactly the same, because of the different properties of protons and carbon ions. For example, carbon Bragg peaks are sharper than those for protons, and they have a forward tail due to carbon fragmentation. In spite, of such differences, the resulting plans are meaningful for our comparison between FDC and GEANT4.

The target volume, prescribed dose, total voxel numbers, voxel size and maximum and minimum energies used in making plan are presented in Table I.

### V. FDC-GEANT4 COMPARISONS

Like in previous studies (Yepes *et al* 2016), we validate FDC by comparing its dose distributions to those obtained with GEANT4, a full-fledged Monte Carlo validated against measurements and widely utilized in the hadron therapy research. Each selected treatment plan is processed with FDC and GEANT4. Both methods are provided with the Radiation Therapy plan, the CT images and the structure in DICOM format from the clinical treatment planning system.

In Table II, we also give the statistical uncertainty of each voxel for Geant4 and FDC, which are shown on the 3rd and 4th column, respectively. The statistical uncertainty is related to the target volumn and number of histories used

Type	Index	Target Volume (cm <sup>3</sup> )	Prescr. Dose (Gy)	Voxel #	Voxel size (mm <sup>3</sup> )	Min Energy (MeV/n)	Max Energy (MeV/n)
Prostate	1	21	65	17,796,597	1.95×1.95×1.0	264	361.26
	2	31	22.0	21,294,338	1.95×1.95×1.0	267.7	381.9
	3	18	38	11,408,683	1.95×1.95×1.25	303	375.5
Brain	1	39	54	12,424,230	1.56×1.56×1.25	137	270.5
	2	63	54	11,195,197	1.56×1.56×1.25	135	294.5
	3	11	55.4	11,967,150	1.95×1.95×1.25	173	250.5
	4	24	50.0	9,564,310	1.95×1.95×1.25	169	278.5
	5	63	30.6	9,026,964	1.95×1.95×1.25	135	247
H & N	1	24	70.0	6,482,515	1.95×1.95×2.5	270.5	346.5
	2	7	66.0	18,624,294	1.95×1.95×1.0	182.5	387.5
	3	14	66.0	22,667,190	1.95×1.95×1.25	219.5	286.5
Lung	1	36	70.0	6,401,252	1.95×1.95×2.5	158	298.5
	2	33	66.0	10,125,024	1.95×1.95×2.5	181	250.5
	3	117	63	5,101,360	2.07×2.07×2.5	204	377
	4	125	66	4,270,560	2.34×2.34×2.5	274.5	387.5
spine	1	138	9.0	23,230,350	1.95×1.95×2.0	237	316.5
	2	48	45.5	6,794,229	1.95×1.95×2.5	209.5	332.5
	3	333	70	10,505,404	1.95×1.95×2.5	135	298
	4	36	50	11,393,369	1.95×1.95×2.5	215.5	312.5

TABLE I: Calculation details for all patients, which include target volume, prescribed dose, total number of voxel and minimum and maximum energies

Type	Index	GEANT 4 $\sigma$	FDC $\sigma$	P <sub>11</sub> (%)	P <sub>22</sub> (%)	P <sub>33</sub> (%)	D <sub>02</sub> (%)	D <sub>05</sub> (%)	D <sub>50</sub> (%)	D <sub>95</sub> (%)	D <sub>98</sub> (%)
Prostate	1	0.396	0.376	96.81	99.82	99.99	0.83	0.66	0.51	0.72	0.73
	2	0.425	0.416	95.82	99.64	99.98	0.91	0.92	0.95	1	1.02
	3	0.378	0.307	95.80	99.61	99.97	1.44	1.45	1.69	1.58	1.42
Brain	1	0.320	0.171	99.70	100.	100.	- 0.52	-0.53	0	0.67	0.79
	2	0.356	0.191	99.67	100.	100.	-0.32	-0.32	0	0.36	0.37
	3	0.314	0.181	99.92	100.	100.	-0.10	-0.20	0.11	0.23	0.23
	4	0.171	0.105	99.95	100.	100.	0.22	0.22	0.12	0.38	0.13
	5	0.417	0.236	99.2	99.98	100.	-0.30	- 0.33	0.59	0	0
H & N	1	0.201	0.112	98.71	99.7	100.	0.85	0.77	0.61	0.66	0.33
	2	0.456	0.334	96.56	99.93	100.	0.5	0.59	1.19	1.38	1.01
	3	0.423	0.181	99.35	99.99	100.	0.58	0.68	0.46	0.91	-0.22
Lung	1	0.335	0.175	99.26	98.99	100.	-0.41	-0.41	-0.09	0.19	0.29
	2	0.273	0.294	95.22	99.67	99.99	1.5	0.86	1.33	1.38	1.41
	3	0.393	0.198	97.63	99.92	100.	0.85	0.67	0.61	0.66	0.33
	4	0.364	0.176	90.28	99.60	99.98	1.23	1.25	1.42	1.43	1.64
spine	1	0.257	0.269	98.42	99.97	100.	0	0	0.73	0	0
	2	0.189	0.141	99.10	99.98	100.	0.51	0.52	0.57	0.16	0.17
	3	0.426	0.207	98.46	99.97	100.	-0.42	-0.34	0.09	0.09	0.1
	4	0.290	0.136	99.93	100.	100.	-0.50	-0.75	-0.67	-0.91	-0.78
RMS		0.35	0.24	97.91	99.83	100.	0.75	0.70	0.79	0.83	0.76

TABLE II: Summary of gamma-index passing rates and difference between the GEANT4 and FDC dosimetric indices for the target volume for all patients. Three different criteria are used for gamma-index calculation: 1%/1mm (P<sub>11</sub>), 2%/2mm (P<sub>22</sub> and 3%/3mm (P<sub>33</sub>). D<sub>02</sub>, D<sub>05</sub>, D<sub>50</sub>, D<sub>95</sub> and D<sub>98</sub> are the maximum dose covering 2%, 5%, 50%, 95% and 98% of the target. Values in the last line are root mean square of all patients.

in the calculation. Higher number of histories will bring down the statistical uncertainty. And larger target volume needs more number of histories to get lower statistical uncertainty.

The statistical uncertainty  $\sigma$  can be calculated in the following steps:

$$\bar{D} = \frac{1}{N} \sum_{i=1}^N D_i$$

$$\sigma = \sqrt{\frac{1}{N} \sum_{i=1}^N (D_i - \bar{D})^2}$$

where  $i$  is the index of the each voxel,  $D_i$  is the dose deposit for each particle in every step in a particular voxel, and  $\bar{D}$  is the mean dose deposit. Note that for those voxels with dose below 10% of the maximum dose are ignored. It requires extra storage space. So it is only kept for voxel energy, then transformed into statistical uncertainty in Dose.

The number of histories is 30 M for each beam when performing FDC calculation. Because the computing time for GEANT4 is usually about 7000 to 18000 times more than FDC, we did not use the same number histories as FDC. The number of histories selected for GEANT4 is to make sure the statistical uncertainty blow 0.4. For all patients discussed in this paper, the number of histories is between 10M to 65M for each beam. As can be noted, by comparing the 6th column with the 5th one, most of the statistical errors for FDC are lower than that for GEANT4 because the number of histories used in FDC is higher than that in Geant4.

We compare the Geant4 and FDC 3D dose distributions by calculating the gamma-index (Low D A, Harms W B, Mutic S and Purdy J A 1998 A technique for the quantitative evaluation of dose distributions Med. Phys. 25 656), which considers both the difference in dose value and spatial position. It is calculated for all voxels with a dose larger than 10% of the maximum dose. We used an algorithm that uses the distance-to-simplex approximation as described in Ju et al 2008 (Ju et al 2008) with the criteria 1%/1 mm, 2%/2 mm and 3%/3 mm. A passing rate is calculated defined as the percentage of voxels that are within the tolerance (gamma index smaller than one).

In addition, we calculate Dose Volume Histograms (DVHs) with FDC and GEANT4 and analyze the difference. DVHs are calculated for structures contoured by physicians. We find that the larger disagreements between FDC and GEANT4 are found for target volumes (TV). We attribute this behavior to the fact that TV are more sensitive to statistical fluctuations than DVHs of Organs at Risk (OAR). Therefore we have concentrated our analysis on this more challenging case of TVs. In order to evaluate the difference in DVHs, we compared D02, D05, D50, D95, and D98, defined as the the maximum dose covering 2%, 5%, 50%, 95% and 98% of volume of the considered structure respectively.

## VI. RESULTS AND DISCUSSION

### A. Dose distribution

The gamma-index analysis is done for all patients with three different criteria, 1 mm/1%, 2 mm/2% and 3 mm/3%. The passing rates with different criteria for all patients were listed in the 5th, 6th and 7th column of Table II. For all the patients, their passing rates are over 90.2% for 1 mm/1%, 98.9% for 2 mm/2% and 99.9% for 3 mm/3%. The RMSs are listed in the last line of Table II, which are 97.91, 99.83 and 100 for different criteria. The high passing rates demonstrate that the FDC dose distributions agree well with that calculated by GEANT 4. These passing rates are visualized in Figure 1, from bottom to top of which are 1 mm/1% (P<sub>11</sub> black dots), 2 mm/2% (P<sub>22</sub>, red squares) and 3 mm/3% (P<sub>33</sub>, green triangles). Figure 1 showed that the cohort of brain, H&N and spine patients have higher gamma-index passing rates than other three types.

We select a head & neck patient (Index 1) as an example to show the FDC-dose, GEANT4-dose and their difference distributions for a specific section in Figure 2. The first plot in this figure is the dose distribution projected in the transverse plane with z=100 mm calculated by FDC. The one in the middle is the dose projection in the same plane from GENAT4. The last panel is the dose difference between two methods (FDC - GEANT4). As shown in the first two plots, the dose distributions simulated by the two methods are similar to each other. Their difference displayed in the last panel shows that the maximum dose difference is of the order of 1 Gy, which confirms that the two methods agree with each other.

The dose distributions in x (lateral), y(anterior-posterior) and z (superior-inferior) projections for all the patients were also compared for a fast evaluation of the agreement. As an example, Figure 3 displays the x, y and z projections for the same patient discussed above. The curves of three projections calculated by the two methods coincide.

### B. Dose-Volume-Histogram

D<sub>02</sub>, D<sub>05</sub>, D<sub>50</sub>, D<sub>95</sub> and D<sub>98</sub> for target volumn for all patients are calculated by GEANT4 and FDC. For each index of DVH, the relative difference between the GEANT4 and FDC values was calculated and listed in columns 8-12 of

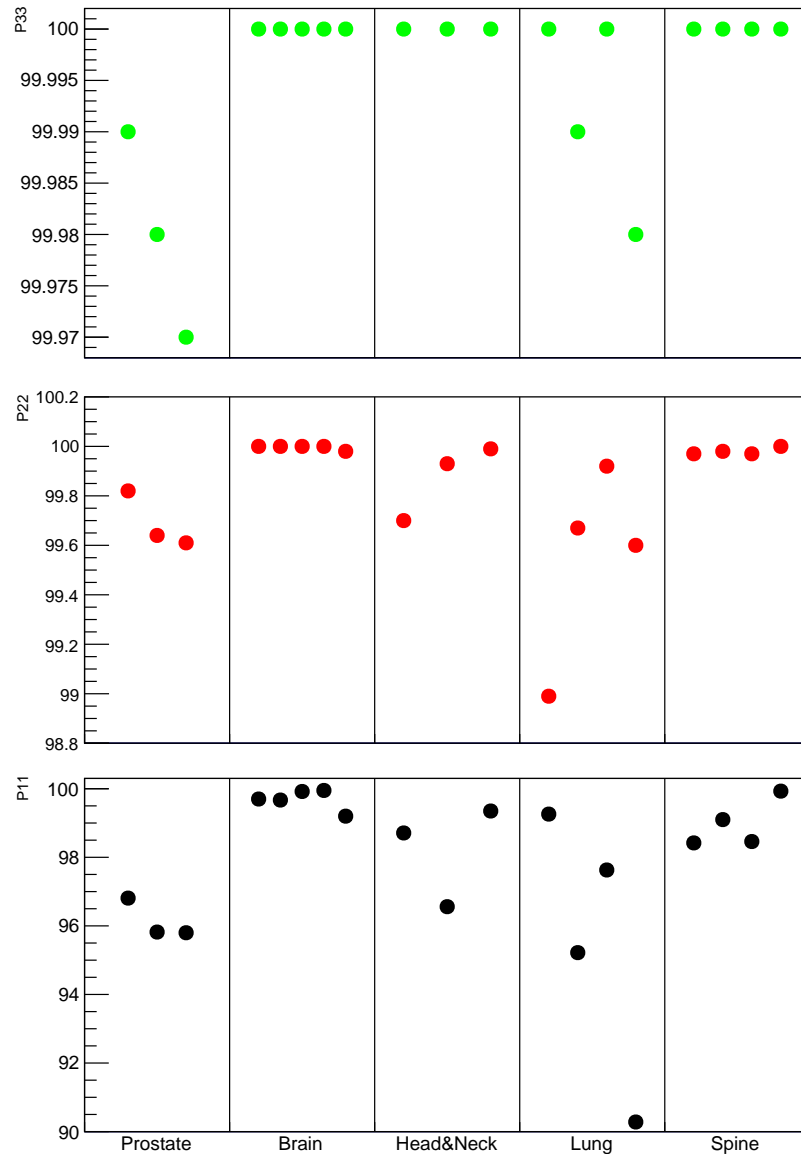


FIG. 1: Gamma-index passing rates for all patients of five different sites studied in this paper. From bottom to top, the criteria used for Gamma-index calculation are 1 mm/1% ( $P_{11}$ , black dots), 2 mm/2% ( $P_{22}$ , red squares) and 3mm/3% ( $P_{33}$ , green triangles).

Table II. The RMS of each index for all patients was calculated and listed in the last line of Table II. The difference in percentage is below 1.5% for D<sub>02</sub>, 1.45% for D<sub>05</sub>, 1.69% for D<sub>50</sub>, 1.58% for D<sub>95</sub> and 1.64 for D<sub>98</sub>. The RMSs of differences in D<sub>02</sub>, D<sub>05</sub>, D<sub>50</sub>, D<sub>95</sub>, D<sub>98</sub> calculated by two codes are 0.75%, 0.70%, 0.79%, 0.83% and 0.76% respectively, which confirm that the DVH calculated by two codes agree well with each other. All these values of difference between GEANT4-DVH and FDC-DVH for target are displayed in Figure 4. The agreement for brain and spine patients is better than the other three types patients, which is consistent with the comparison of dose distribution.

Figure 5 displays DVHs of the same head & neck patient mentioned above for four selected structures: GTV (black), Hypothalamus (red), Brain.Stem (green) and Frontal.Lobe (light blue). The open squares and solid line are for FDC and GEANT4 calculations, respectively. The comparisons show that the DVHs calculated by the two methods agree well with each other. Especially, the DVHs for Brain.Stem and Frontal.Lobe from the two methods are virtually indistinguishable.

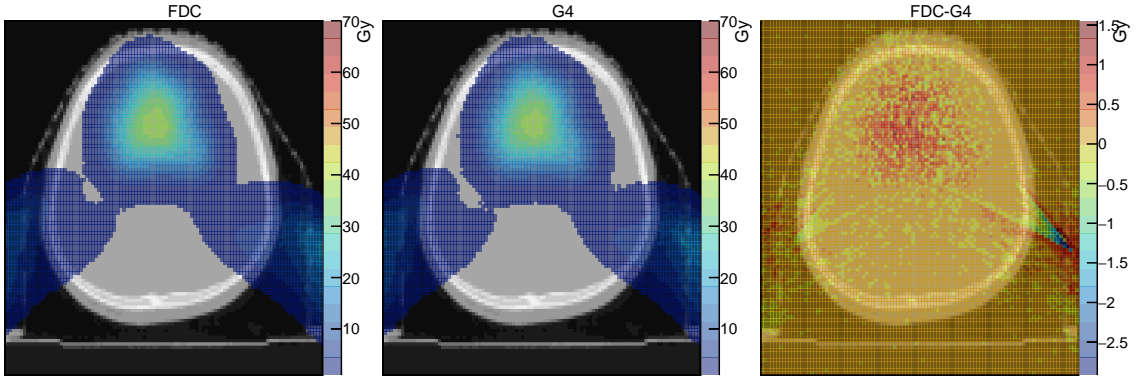


FIG. 2: Gamma-index passing rates for all patients of five different sites studied in this paper. From bottom to top, the criteria used for gamma-index calculation are 1 mm/1% ( $P_{11}$ , black dots), 2 mm/2% ( $P_{22}$ , red squares) and 3mm/3% ( $P_{33}$ , green triangles).

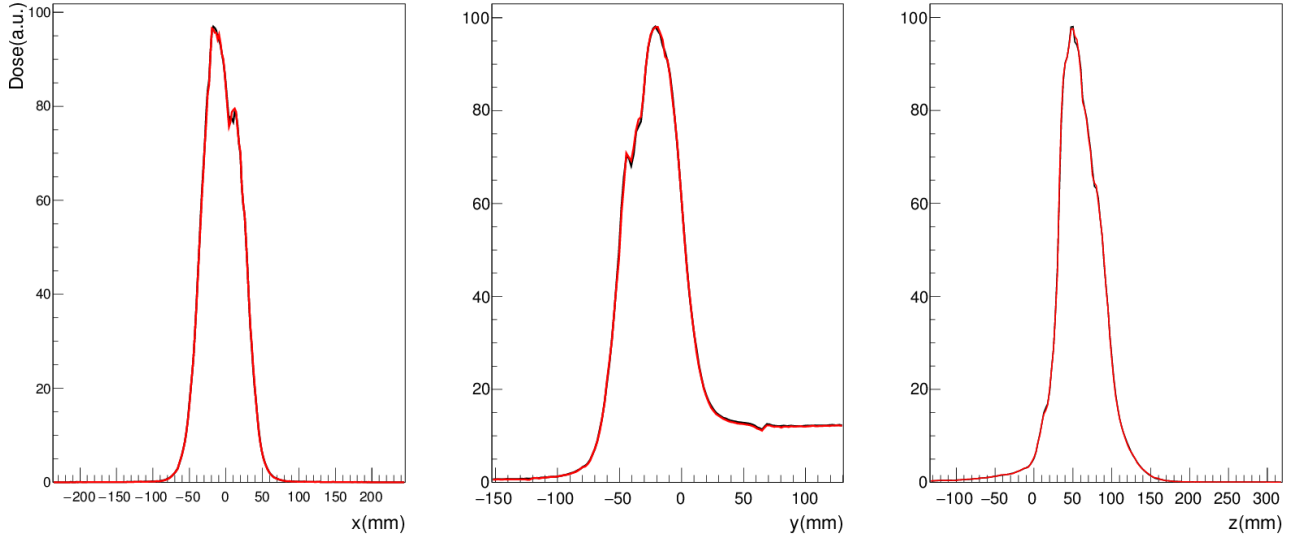


FIG. 3: Dose distribution projection in the direction superior to inferior (x), left to right (y) and anterior to posterior (z) for the same patient calculated by FDC (black line) and GEANT4 (red line)).

## VII. CONCLUSIONS

In this paper, we used GEANT 4, a widely used full-fledged Monte Carlo code as the standard to verify the accuracy of the Fast Dose Calculator (FDC) code in carbon patients calculation. We compared dose distributions and dose-volume-histograms (DVH) calculated by FDC and GEANT4. The gamma-index passing rates with the criterion 2%/2 mm are above 98.5% for all patients, and the passing rates are above 99.9 for all patients if 3%/3 mm is used. For DVH, the Root Mean Square (RMS) for the difference of five selected slices ( $D_{02}$ ,  $D_{05}$ ,  $D_{50}$ ,  $D_{95}$ ,  $D_{98}$ ) calculated by FDC and GEANT4 are below 0.75%, 0.70%, 0.79%, 0.83% and 0.76% respectively. Therefore, the FDC accuracy amply satisfies the requirement for clinical use.

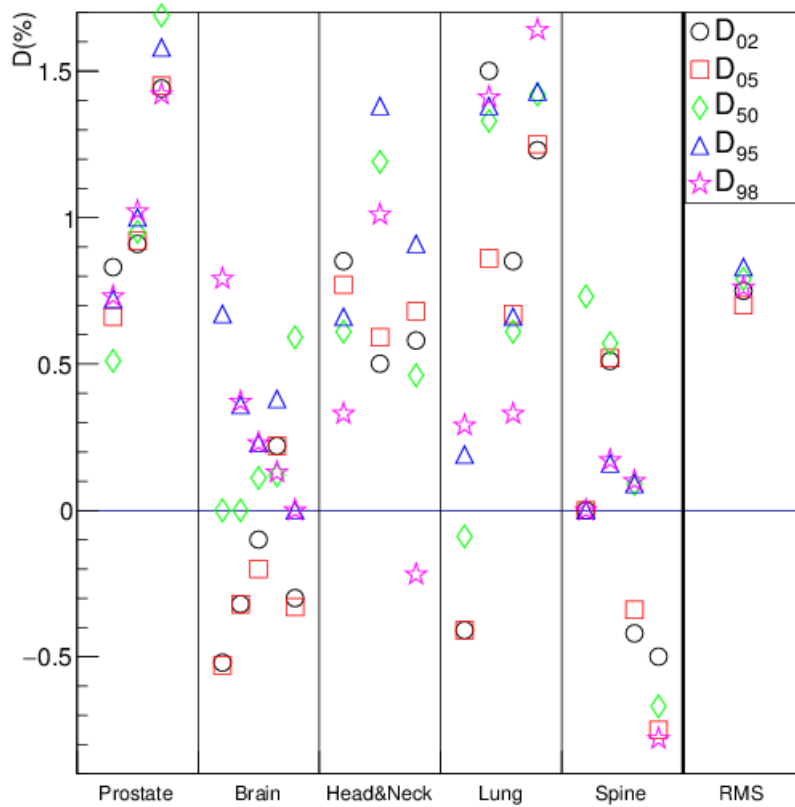


FIG. 4: Difference of five different indices of target volume DVH:  $D_{02}$ ,  $D_{05}$ ,  $D_{50}$ ,  $D_{95}$ , and  $D_{98}$ . Negative difference means FDC-DVH is small than GEANT4-DVH.

## VIII. ACKNOWLEDGEMENT

- 
- Agostinelli S et al 2003 GEANT4a simulation toolkit Nucl. Instrum. Methods A 506 250-303.  
Allison J et al 2006 Geant4 developments and applications IEEE Trans. Nucl. Sci. 53 270-8.  
Amaldi U and Kraft G 2005 Radiotherapy with beams of carbon ions Rep. Prog. Phys. 68 1861-82.  
Castro J R, Petti P L, Blakely E A and Daftari I K 2004 Particle radiation therapy Textbook of Radiation Oncology S A Leibel and T L Phillips (Philadelphia, PA/Amsterdam: Saunders/Elsevier) pp 1547-68.  
Deasy J O 1998 A proton dose calculation algorithm for conformal therapy simulations based on Moliere theory of lateral deceptions Med. Phys. 25 476-83.  
Hong L, Goitein M, Bucciolini M, Comiskey R, Gottschalk B, Rosenthal S, Serago C and Urie M 1996 A pencil beam algorithm for proton dose calculations Phys. Med. Biol. 41 1305-30  
Kraft G 2000 Tumor Therapy with Heavy Charged Particles Prog. Part. Nucl. Phys. 45 S473-544.  
Newhauser W D, Zhang R 2015 The physics of proton therapy Phys. Med. Biol. 60 R155-209  
Ohno T Particle radiotherapy with carbon ion beams. EPMA J 2013 4-9.  
Petti P L 1992 Differential-pencil-beam dose calculations for charged particles Med. Phys. 19 137-49  
Poludniowski G, Allinson N M and Evans P M 2015 Proton radiography and tomography with application to proton therapy Br. J. Radiol. 88 20150134.  
Particle Therapy Cooperative Group (PTCOG) webpage (<https://www.ptcog.ch/>).  
Russell K R, Grusell E and Montelius A 1995 Dose calculations in proton beams: range straggling corrections and energy

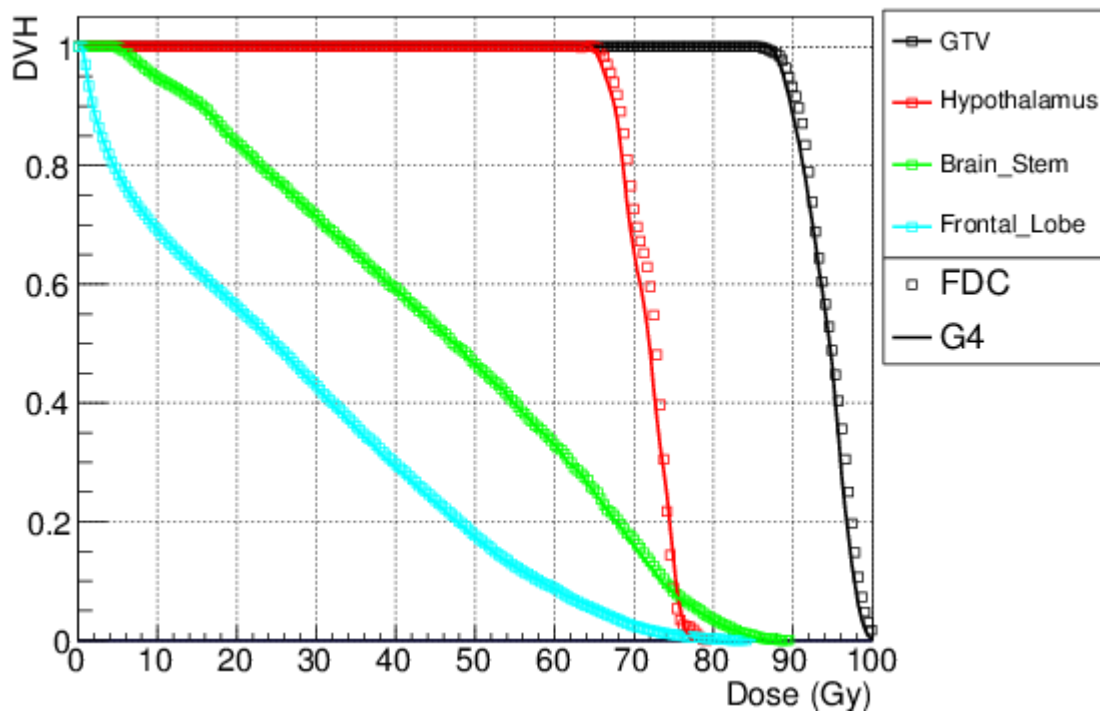


FIG. 5: Dose-volume histograms of a head & neck patient (Index 1) calculated with FDC and GEANT4.

scaling Phys. Med. Biol. 40 1031-43.

Schaffner B, Pedroni E and Lomax A 1999 Dose calculation models for proton treatment planning using a dynamic beam delivery system: an attempt to include density heterogeneity effects in the analytical dose calculation Phys. Med. Biol. 44 27-41.

Szymanowski H and Oelfke U 2002 Two-dimensional pencil-beam scaling: an improved proton dose algorithm for heterogeneous media Phys. Med. Biol. 47 3313-30.

Schulz-Ertner D, *et al* 2004 Results of carbon ion radiotherapy in 152 patients Int. J. Radiat. Biol. Phys. 58 631-40.

Schulz-Ertner D, Tsujii H. 2007 Particle radiation therapy using proton and heavier ion beams J. Clin. Oncol. 25 953-64.

Schneider U, Schaffner B, Lomax A J, Pedroni E and Tourovsky A 1998 A technique for calculating range spectra of charged particle beams distal to thick inhomogeneities Med. Phys. 25 457-63

Taylor P A, Kry S and Followill D 2017 Pencil beam algorithms are unsuitable for proton dose calculations in lung Int. J. Radiat. Oncol. 99 750-6

Tsujii H *et al* 2004 Overview of clinical experience on carbon ion therapy at NIRS Radiother. Oncol. 73 S41-9.

Wilson R R 1946 Radiological use of fast protons Radiology 47 487-91

Yepes P, Brannan T, Huang J, Mirkovic D, Newhauser W D, Taddei P J and Titt U 2010b Application of a fast proton dose calculation algorithm to a thorax geometry Radiat. Meas. 45 1367-8

Yepes P, Eley J G, Liu A, Mirkovic D, Randeniya S, Titt U and Mohan R 2016 Validation of a track repeating algorithm for intensity modulated proton therapy: clinical cases study Phys. Med. Biol. 61 2633-45

Yepes P, Mirkovic D and Taddei P 2010a GPU implementation of a track-repeating algorithm for proton radiotherapy dose calculations Phys. Med. Biol. 55 7107-20

Yepes P, Randeniya S, Taddei P J and Newhauser W D 2009a A track repeating algorithm for fast Monte Carlo dose calculations of proton radiotherapy Nucl. Technol. 168 334-7

Yepes P, Randeniya S, Taddei P J and Newhauser W D 2009b Monte Carlo fast dose calculator for proton radiotherapy: application to a voxelized geometry representing a patient with prostate cancer Phys. Med. Biol. 54 N21-8